Tutorial

Theory and Application of Radiation Boundary Operators

THOMAS G. MOORE, STUDENT MEMBER, IEEE, JEFFREY G. BLASCHAK, STUDENT MEMBER, IEEE, ALLEN TAFLOVE, SENIOR MEMBER, IEEE, AND GREGORY A. KRIEGSMANN

Invited Review Paper

***Abstract*—A succinct unified review is provided of the theory of radiation boundary operators which has appeared principally in the applied mathematics and computational physics literature over the last ten years. With the recent introduction of the on-surface radiation condition (OSRC) method and the continued growth of finite-difference and finite-element techniques for modeling electromagnetic wave scattering problems, the understanding and use of radiation boundary operators has become increasingly important to the engineering community. In the OSRC method, specific radiation boundary operators are applied directly on the surface of an arbitrary convex target, substantially simplifying the usual integral equation for the scattered field. In the finite-difference and finite-element techniques, radiation boundary operators are used to truncate the computational domain near the target, while accurately simulating an infinite modeling space. Results are presented to illustrate the application of radiation boundary operators in both of these areas. Recent OSRC results include analysis of the scattering behavior of both electrically small and electrically large cylinders, a reactively loaded acoustic sphere, and a simple reentrant duct. New radiation boundary operator results include the demonstration of the effectiveness of higher order operators in truncating finite-difference time-domain grids.**

I. Introduction

WITH THE RECENT introduction of the on-surface radiation condition (OSRC) method [1] and the continued growth of finite-difference time-domain (FD-TD) [2] and finite-element [3] techniques for modeling electromagnetic wave scattering problems, the understanding and use of radiation boundary operators has become increasingly important to the engineering community. Radiation boundary operators have fundamentally different uses in the OSRC and finite-difference/finite-element methods. Finite techniques use radiation boundary operators in either the time domain or frequency domain to create a radiation boundary condition (RBC) which truncates a volumetric computational domain electrically close to a modeled target, and yet effectively simulates the extension of the computational domain to infinity. In contrast, the OSRC method uses the radiation boundary operator directly on the surface of the target to reduce the usual frequency-domain integral equation for the scattered field to either an integration of known quantities or a second-order ordinary differential equation. Each is simply implemented on the target surface. Although the OSRC and finite methods use radiation boundary operators in different manners, both techniques can be greatly enhanced by more effective radiation boundary operators.

The purpose of this paper is to provide a succinct unified review of key research that has been performed in the area of radiation boundary operators. Because much of this research has appeared in the applied mathematics and computational physics literature over the past ten years, its results and implications are generally not well known by the engineering electromagnetics community. This paper will also present some recent results from the application of these operators to engineering problems. In particular, we will examine two basic types of radiation boundary operators and give examples showing their use in both the FD-TD and OSRC methods. Specifically, in Section II we will discuss the theory behind radiation boundary operators. In Section III the radiation boundary operators will be used to construct new radiation boundary conditions for a two-dimensional FD-TD grid of higher order than those currently used; and the effectiveness of the new radiation boundary conditions will be tested. In Section IV, the radiation boundary operators will be used in the OSRC method to approximately solve the problem of scattering from a perfectly conducting cylinder. Section V concludes with a discussion of the research activities that are ongoing in the areas of radiation boundary operators and their applications.

II. Theory

There are two basic types of radiation boundary operators: mode annihilating and one-way wave equation approximations. Each of these radiation boundary operators possesses different characteristics and forms. In this section, the two different types of radiation boundary operators are examined in detail.

Manuscript received October 15, 1987; revised January 18, 1988. This work was supported in part by NASA Lewis Research Center Grant NAG 3-635 and in part by the National Science Foundation Grant MCS-8300578.

T. G. Moore and A. Taflove are with the Department of Electrical Engineering and Computer Science, Technological Institute, Northwestern University, Evanston, IL 60201.

J. G. Blaschak is with the Lincoln Laboratory, Massachusetts Institute of Technology, Lexington, MA 02173.

G. A. Kriegsmann is with the Department of Engineering Sciences and Applied Mathematics, Technological Institute, Northwestern University, Evanston, IL 60201.

IEEE Log Number 8823652.

A. Mode-Annihilating Operators

The first type of radiation boundary operator to be discussed is the mode-annihilating differential operator. This type of operator is based on the idea of killing the terms (herein referred to as "modes") of the far-field expansion of outward propagating solutions to the wave equation. One can view the idea of killing modes of the scattered fields as first being proposed by Sommerfeld in the form of the Sommerfeld radiation condition [4] which annihilates the first mode in the expansion. Later, researchers [5] extended the Sommerfeld theory and created an operator that annihilates the next mode in the expansion. Independently, other researchers created a general operator that kills an arbitrary number of modes in the expansion as derived and presented in [6]. It is the theory that appeared in [6] that will be reviewed in this section.

For this section we will proceed as follows. In Section II-A1) the scattered fields are written in terms of a far-field expansion, and the effect that the Sommerfeld radiation condition has on the expansion is presented. The operators derived in [6], are presented in Section II-A2) for the full three-dimensional case and are specialized to two dimensions in Section II-A3).

1) Far-Field Expansions and the Sommerfeld Radiation Condition: We consider here solutions $U(R, \theta, \phi, t)$ to the scalar wave equation

$$\nabla^2 U - U_{tt} = 0 \tag{1}$$

and the associated Helmholtz equation for time-harmonic waves

$$\nabla^2 U + k^2 U = 0 \tag{2}$$

where the wave speed c has been scaled to unity and the harmonic wave is assumed to have time dependency $e^{-j\omega t}$. The radiating solutions of the scalar wave equation (i.e., solutions propagating in directions which are outward from the origin of a spherical coordinate system) can be expanded in a convergent series of the form [7],

$$U(R, \theta, \phi, t) = \sum_{i=1}^{\infty} \frac{f_i(t-R, \theta, \phi)}{R^i}. \tag{3}$$

This result was extended to the time-harmonic case for both vector and scalar fields [8]. For the scalar Helmholtz equation, it is proved in [8] that

$$U(R, \theta, \phi) = \frac{e^{jkR}}{R} \sum_{i=0}^{\infty} \frac{f_i(\theta, \phi)}{R^i} \tag{4}$$

is a convergent expansion for scalar wave functions that satisfy the Sommerfeld radiation condition.

The Sommerfeld radiation condition [4], given by

$$\lim_{R\to\infty} R(U_R - jkU) = 0 \tag{5a}$$

where U_R denotes a derivative respect to R, is satisfied by the each term of (4). By using the correspondence $-jk = \partial/\partial t$, the Sommerfeld condition is extended to

$$\lim_{R\to\infty} R(U_R + U_t) = 0 \tag{5b}$$

which is satisfied by each term of the expansion in (3). The Sommerfeld radiation condition can be viewed as an operator on the far-field expansion of U giving the asymptotic result,

$$\left(\frac{\partial}{\partial R} - jk\right) U = O(R^{-2}) \tag{6}$$

in the limit $R \to \infty$. In other words, the Sommerfeld condition retains terms that are no greater than $O(R^{-2})$ in the expansion.

2) Higher Order Operators: With the goal of devising operators that annihilate terms up to any order in the far-field expansion of U, a sequence of operators B_n was proposed [6] for the expansion in (3). A similar sequence of operators was independently developed for the Helmholtz equation in two dimensions [5]. The former were extended [9] for the Helmholtz equation in both two and three dimensions. We restrict our review here to operators for the time-harmonic case [9], keeping in mind that results for waves of arbitrary time variation can be obtained by a simple substitution of $\partial/\partial t$ for the term $-jk$.

The derivation of B_n begins by multiplying a slightly rewritten version of (4) by R^n and then splitting the sum as shown:

$$R^n U(R, \theta, \phi) = \sum_{i=1}^{n} R^{n-i} e^{jkR} F_i(\theta, \phi) + \sum_{i=n+1}^{\infty} R^{n-i} e^{jkR} F_i(\theta, \phi). \tag{7}$$

Now define the intermediate operator,

$$L \equiv \frac{\partial}{\partial R} - jk \tag{8a}$$

and observe that applying L^n to both sides of (7) annihilates the first sum and makes the leading order term of the second sum be $O(R^{-n-1})$. We have

$$L^n(R^n U) = O(R^{-n-1}) \tag{8b}$$

which accomplishes the goal of annihilating the first n terms of the far-field expansion. A more useful way to express this result is as a single operator acting on U only. This is achieved by inductive arguments [9]. For $n = 1$,

$$L(RU) = \left(\frac{\partial}{\partial R} - jk\right) RU = O(R^{-2}) \tag{9a}$$

$$R\left(\frac{\partial}{\partial R} - jk\right) U + U = O(R^{-2}) \tag{9b}$$

which can be written as

$$\left(\frac{\partial}{\partial R} - jk + \frac{1}{R}\right) U = O(R^{-3}). \tag{9c}$$

The first operator in the sequence is then

$$B_1 = L + \frac{1}{R} \tag{10a}$$

which, when applied to both sides of (4), annihilates the first term of the expansion. Similarly,

$$B_2 = \left(L + \frac{3}{R}\right)\left(L + \frac{1}{R}\right) \tag{10b}$$

annihilates the first two terms. In general, the recursion relation,

$$B_n = \left(L + \frac{2n-1}{R}\right) B_{n-1} \tag{11}$$

produces an operator which annihilates the first n terms of the expansion in (4). The sequence of operators gives

$$B_n U = O(R^{-2n-1}) \tag{12}$$

for any function U satisfying the expansion in (4).

In the literature, B_n has been utilized as a boundary condition

$$B_n U = 0 \tag{13}$$

for the wave function U. This condition becomes more accurate, in powers of R^{-1}, as the order of the operator n increases. The original application of (13) was to truncate a computational domain while accurately modeling the outward propagation of waves to infinity. Further application of B_n, particularly B_2, is found in the OSRC method for computing scattering from two-dimensional, convex, conducting and homogenous dielectric bodies.

3) Operators for Two-Dimensional Wave Propagation: Extension of B_n for use with wave functions $U(r, \theta, t)$ in two space dimensions proceeds in the time harmonic case from an expansion presented in [10],

$$U(r, \theta) = H_0(kr) \sum_{i=0}^{\infty} \frac{F_i(\theta)}{r^i} + H_1(kr) \sum_{i=0}^{\infty} \frac{G_i(\theta)}{r^i} \tag{14}$$

which has the far-field result [9],

$$U(r, \theta) = \sqrt{\frac{2}{\pi kr}}\, e^{j(kr-(\pi/2))} \sum_{i=0}^{\infty} \frac{f_i(\theta)}{r^i} \tag{15}$$

that is analogous to (4). A sequence of boundary operators is defined [6] by the recursion relationship

$$B_n = \left(L + \frac{4n-3}{2r}\right) B_{n-1} \tag{16}$$

where

$$B_1 = L + \frac{1}{r} \tag{17a}$$

and

$$L \equiv \frac{\partial}{\partial r} - jk. \tag{17b}$$

The operator B_n annihilates the first n terms of the expansion (16) and yields

$$B_n U = O(r^{-2n-1/2}). \tag{18}$$

The utility of these operators will be demonstrated in Section IV in the OSRC calculation of electromagnetic scattering from a conducting circular cylinder illuminated by a TE polarized plane wave. The first two operators used there are

$$B_1 = \frac{\partial}{\partial r} + \frac{1}{2r} - jk \tag{19a}$$

and

$$B_2 = \frac{\partial}{\partial r} + \frac{1}{2r} - jk - \left(\frac{\partial^2}{\partial \theta^2} + \frac{1}{4}\right) \Big/ \left[2r^2 \left(\frac{1}{r} - jk\right)\right]. \tag{19b}$$

In the derivation of (19b) the recursion relation, (16) produces a second-order r derivative. It is conveniently eliminated by the substitution from the Helmholtz equation,

$$\frac{\partial^2}{\partial r^2} = -\frac{1}{r^2}\frac{\partial^2}{\partial \theta^2} - \frac{1}{r}\frac{\partial}{\partial r} - k^2. \tag{20}$$

B. One-Way Wave Equations

A partial differential equation which permits wave propagation only in certain directions is called a "one-way wave equation." Fig. 1 shows a finite two-dimensional Cartesian domain Ω on which the time-dependent wave equation is to be simulated. In the interior of Ω, a numerical scheme which models wave propagation in all directions is applied. On the outer boundary $\partial\Omega$, only numerical wave motion that is outward from Ω is permitted. The boundary must permit outward propagating numerical waves to exit Ω just as if the simulation were performed on a computational domain of infinite extent. A scheme which enacts a one-way wave equation on $\partial\Omega$ for this purpose is called a radiation boundary condition (RBC).

1) Derivation by Wave Equation Factoring[1]*:* The derivation of an RBC whose purpose is to absorb numerical waves incident upon the outer boundary of a finite-difference or finite-element grid can be explained in terms of operator factoring. Consider the two-dimensional wave equation in Cartesian coordinates,

$$U_{xx} + U_{yy} - U_{tt} = 0. \tag{21}$$

The partial differential operator here is

$$L \equiv D_x^2 + D_y^2 - D_t^2 \tag{22a}$$

which uses the notation,

$$D_x^2 \equiv \frac{\partial^2}{\partial x^2} \qquad D_y^2 \equiv \frac{\partial^2}{\partial y^2} \qquad D_t^2 \equiv \frac{\partial^2}{\partial t^2}. \tag{22b}$$

The wave equation is then compactly written as

$$LU = 0. \tag{23}$$

The wave operator L can be factored in the following manner:

$$LU = L^+ L^- U = 0 \tag{24a}$$

[1] It can be demonstrated that wave equation factoring can generate B_1 and B_2 described in Section II-A. However, this has not been shown for $n > 2$.

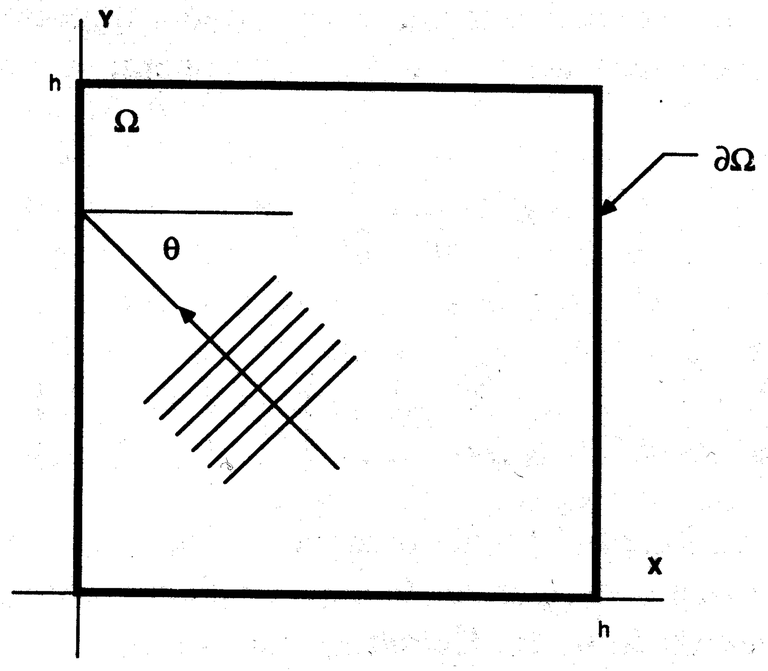

Fig. 1. Two-dimensional Cartesian computational domain.

where L^- is defined as

$$L^- \equiv D_x - D_t\sqrt{1-S^2} \tag{24b}$$

with

$$S=\frac{D_y}{D_t}. \tag{24c}$$

the operator L^+ is similarly defined except for a "+" sign before the radical.

In [11] it is shown that at a boundary, say at $x = 0$, the application of L^- to the wave function U will exactly absorb a plane wave incident at any angle and traveling in the $-x$ direction. Thus

$$L^- U=0 \tag{25}$$

applied at $x = 0$ functions as an exact analytical RBC which absorbs wave motion from the interior of the spatial domain $\{\Omega = (x, y):0 < x < h, 0 < y < h\}$. The operator L^+ performs the same function for waves traveling in the $+x$ direction that impact the other x boundary in Fig. 1 at $x = h$. The presence of the radical in (24b) classifies L^- as a pseudodifferential [11] operator that is nonlocal in both the space and time variables. This is an undesirable characteristic in that it prohibits the direct numerical implementation of (25) as an RBC.

Approximation of the radical in (24b) produce RBC's that can be implemented numerically and are useful in FD-TD simulations of the wave equation. The numerical implementation of an RBC is not exact in that a small amount of reflection does develop as numerical waves pass through the grid boundary. However, it is possible to design an RBC which minimizes the reflection as much as possible over a range of incident angles [12]. The RBC derived in [13] and applied in the simulation of electromagnetic scattering [14], uses a two-term Taylor series approximation to the radical in (24b).

$$\sqrt{1-S^2}\approx 1-\frac{1}{2}S^2. \tag{26a}$$

This leads to the following approximate analytical RBC which can be numerically implemented at the $x = 0$ boundary:

$$U_{xt}-U_{tt}+\frac{1}{2}U_{yy}=0. \tag{26b}$$

A generalization of (26) presented in [15] showed that the construction of numerically useful absorbing boundary conditions reduces to approximation of $\sqrt{1 - S^2}$ on the interval $[-1, 1]$ by the rational function,

$$r(s)=\frac{p_m(s)}{q_n(s)} \tag{27}$$

where p and q are polynomials of degree m and n, and $r(s)$ is said to be of type (m, n). By specifying $r(s)$ as a general type (2, 0) approximant, the radical is approximated by an interpolating polynomial of the form

$$\sqrt{1-S^2}\approx p_0+p_2S^2 \tag{28a}$$

resulting in the general second-order approximate analytical RBC,

$$U_{xt}-p_0U_{tt}-p_2U_{yy}=0. \tag{28b}$$

The choice of the coefficients p_0 and p_2 is determined by the method of interpolation. Standard techniques such as Chebyshev, least-squares, or Padé approximation are applied with the goal of producing an approximate RBC whose performance is good over a wide range of incident wave angles. Expressions similar to (28) can be derived and applied at the other three boundaries of a two-dimensional FD-TD grid.

High order approximations to the radical in (24b) were proposed in [15] as a means to derive a more accurate approximate RBC. Use of the general type (2, 2) rational function,

$$\sqrt{1-S^2}\approx\frac{p_0+p_2S^2}{q_0+q_2S^2} \tag{29a}$$

gives the general third-order approximate analytical RBC,

$$q_0U_{xtt}+q_2U_{xyy}-p_0U_{ttt}-p_2U_{tyy}=0. \tag{29b}$$

Appropriate selection of the p and q coefficients in (29) produces various families of RBC's, as suggested in [12] and [15]. For example, $q_0 = p_0 = 1, p_2 = -3/4$, and $q_2 = -1/4$ gives a Padé (2, 2) approximation in (29a) with the resulting RBC function better than (26b) for numerical waves impacting the grid boundary at near normal incidence. This results in the third-order RBC originally proposed in [11]. Other types of approximating polynomials "tune" the RBC to absorb numerical waves incident at specified angles other than normal, and are considered to be a means to improve wide-angle performance [12]. Results from a comparative study [16] of the performance of various families of RBC's are presented in Section III.

2) Derivation by Dispersion Relation: An alternate procedure for obtaining one-way wave equations is presented in the literature [12], [15]. We summarize the technique here for completeness. It is well known that if the dispersion

relation for a linear constant-coefficient partial differential equation is known, then the equation itself is specified [17]. Thus if one can obtain the dispersion relation for a one-way wave equation, then an RBC appropriate for use on $\partial\Omega$ is obtained.

If a plane wave solution

$$U(x, y, t) = e^{j(\omega t + \xi x + \eta y)} \tag{30}$$

is substituted into (21), then

$$\omega^2 = \xi^2 + \eta^2 \tag{31}$$

is the dispersion relation for the wave equation which permits wave propagation in all directions of the x–y plane. The wave in (30) has velocity

$$\mathbf{v} = v_x \hat{\mathbf{x}} + v_y \hat{\mathbf{y}} \tag{32a}$$

where

$$v_x = -\frac{\xi}{\omega} = -\cos\theta \tag{32b}$$

$$v_y = -\frac{\eta}{\omega} = -\sin\theta \tag{32c}$$

and θ is the counterclockwise angle measured from the the negative x axis. By rewriting (31) as

$$\frac{\xi}{\omega} = \pm\sqrt{1 - s^2} \tag{33a}$$

with

$$s = \frac{\eta}{\omega} \tag{33b}$$

a dispersion relation can be identified which corresponds to an equation that admits plane wave solutions propagating only in the $-x$ direction. This is obtained by choosing the positive branch of the square root in (33a) which corresponds to waves having velocity component v_z, in the $-x$ direction. Wave motion from the interior of Ω will be absorbed at the $x = 0$ grid boundary if an equation having the dispersion relation,

$$\xi = \omega\sqrt{1 - s^2}. \tag{34}$$

is applied at that boundary.

Equation (34) is a dispersion relation for a pseudodifferential equation [11] and cannot be identified with a linear partial differential equation which can be implemented numerically on the $x = 0$ boundary. By approximating the radical in (34), it is possible to obtain a dispersion relation which can be identified with a partial differential equation that functions as an approximate analytical RBC. The same methods of approximation for the radical used in Section II-A1) can be applied here; however, s is now defined by (33b). Once a dispersion relation is obtained with approximates the exact relation in (34), the same RBC's are derived as in Section II-A1). We illustrate here application of the two-term Taylor series approximation to the radical. Equation (34) becomes

$$\xi = \omega\left(1 - \frac{1}{2}\frac{\eta^2}{\omega^2}\right) \tag{35a}$$

which is equivalent to

$$\xi\omega = \omega^2 - \frac{1}{2}\eta^2 \tag{35b}$$

which is the dispersion relation of

$$U_{xt} = U_{tt} - \frac{1}{2}U_{yy}. \tag{35c}$$

This is the same expression as the approximate analytical RBC given in (26b). Higher order RBC's follow directly.

III. Application of One-Way Wave Equations: FD-TD Radiation Boundary Conditions

In the simulation of electromagnetic wave scattering by finite techniques, one-way wave equations are used to truncate the computational domain in a manner which accurately models the propagation of scattered waves to infinity [13], [14]. This section summarizes recent results in applying the theory of one-way wave equations to the simulation of electromagnetic scattering by the FD-TD method. In particular, the promise of higher order RBC's is quantified by a reflection coefficient analysis and by numerical experiments. It is demonstrated that a reduction in grid boundary reflection is realized when a third-order RBC is applied on the boundary of a two-dimensional FD-TD grid.

A. Reflection Coefficient Analysis

Numerical radiation boundary conditions derived from approximate analytical one-way wave equations are not exact in that a small amount of reflection will be realized from numerical wave striking the grid boundary. For a numerical plane wave striking the $x = 0$ boundary in Fig. 1, the amount of reflection is dependent upon the angle of incidence θ. Now, scattered waves from a complex body can be viewed as a superposition of plane waves striking the computational boundaries over a wide range of incident angles. Therefore, the performance of a given RBC can be assessed by deriving a reflection coefficient R, which quantifies the amount of nonphysical reflection a plane wave produces as a function of θ when it interacts with the grid boundary. Clearly, a good RBC gives a small value of R over a wide range of θ. Such an RBC should perform well in the simulation of a realistic scattering situation because the grid boundaries would permit most of the scattered energy to exit the computational domain.

Consider the outgoing plane wave in Fig. 1. The wave has the form,

$$U_{\text{inc}} = e^{j(kt + kx\cos\theta - ky\sin\theta)}. \tag{36}$$

The total field at the boundary of the computational domain must satisfy the specific RBC in effect there. Postulating the existence of a reflected wave launched from the boundary, the

TABLE I
COEFFICIENTS FOR THIRD-ORDER RBC'S

Type of Approximation	p_0	p_2	q_2	Angles of Exact Absorption (°)
Padé	1.00000	−0.75000	−0.25000	0.00
L_a^∞	0.99973	−0.80864	−0.31657	11.7, 31.9, 43.5
Chebyshev points	0.99650	−0.91296	−0.47258	15.0, 45.0, 75.0
L^2	0.99250	−0.92233	−0.51084	18.4, 51.3, 76.6
C-P	0.99030	−0.94314	−0.5556	18.4, 53.1, 81.2
Newman points	1.00000	−1.00000	−0.66976	0.0, 60.5, 90.0
L^∞	0.95651	−0.94354	−0.70385	26.9, 66.6, 87.0

$q_0 = 1.00000$ for each technique.

TABLE II
COEFFICIENTS FOR SECOND-ORDER RBC'S

Type of Approximation	p_0	p_2	Angles of Exact Absorption (°)
Padé	1.00000	−0.50000	0.00
L_a^∞	1.00023	−0.51555	7.6, 18.7
Chebyshev points	1.03597	−0.76537	22.5, 67.5
L^2	1.03084	−0.73631	22.1, 64.4
C-P	1.06103	−0.84883	25.8, 73.9
Newman points	1.00000	−1.00000	0.0, 90.0
L^∞	1.12500	−1.00000	31.4, 81.6

total field at the $x = 0$ boundary has the form,

$$U = e^{j(kt + kx\cos\theta - ky\sin\theta)} + Re^{j(kt - kx\cos\theta - ky\sin\theta)} \tag{37}$$

where R can be determined by substituting U directly into the equation for the RBC used at the $x = 0$ boundary.

By substituting (37) into (28b) and (29b), reflection coefficient expressions as a function of incident angle are obtained for the general second- and third-order RBC's. They are, respectively,

$$R = \frac{\cos\theta - p_0 - p_2\sin^2\theta}{\cos\theta + p_0 + p_2\sin^2\theta} \tag{38}$$

and

$$R = \frac{q_0\cos\theta + q_2\cos\theta\sin^2\theta - p_0 - p_2\sin^2\theta}{q_0\cos\theta + q_2\cos\theta\sin^2\theta + p_0 + p_2\sin^2\theta} \tag{39}$$

where the coefficients p and q correspond to the approximating function used in the derivation of the RBC. Seven techniques of approximation are developed in [15] for this purpose. The techniques are: Padé; Chebyshev on a subinterval (L_a^∞); interpolation in Chebyshev points; least-squares (L^2); Chebyshev–Padé (or C–P); interpolation in Newman points; and Chebyshev (L^∞). Tables I and II show p and q coefficients for approximating functions of both second and third order. The mechanics of their derivation can be found in [15]. A type (2, 2) approximant produces a third-order RBC. Second-order RBC's are obtained from type (2, 0) approximants. Also shown in Tables I and II are angles of incidence at which the RBC's are designed to exactly absorb numerical plane waves. The Padé family concentrates absorption near $\theta = 0°$. The others distribute absorption angles through the range $[0, \pi/2]$ as a means to improve wide-angle performance [15]. A more general approach, which permits the design of boundary conditions for plane waves incident at arbitrary angles, is presented in [18] and [19].

Figs. 2 and 3 show the behavior of the reflection coefficient for the two best-performing RBC's as a function of incident angle on the range $[0, \pi/2]$. In all cases studied, the behavior of reflection coefficient for third-order RBC's is better than that of second-order RBC's. Fig. 2(a) shows R less than one percent for $0 < \theta < 45°$ for the third-order Padé RBC. Note that the Padé RBC's have a very low reflection coefficient for normal incidence. The distribution of exact absorption angles away from $\theta = 0°$ is illustrated in Fig. 2(b) for the L_a^∞ RBC. The nulls in the behavior of R are as predicted by the analysis presented in [15]. Fig. 3 compares the third-order Padé and the third-order L_a^∞ RBC's. By sacrificing performance near $\theta = 0°$, the L_a^∞ RBC extends the point at which R is less than one percent to about $\theta = 60°$.

B. Numerical Experiments

Numerical experiments are now reported which clearly measure the amount of nonphysical reflection a given RBC produces as a pulse propagates through a grid boundary. Fig. 4(a) shows two domains on which the two-dimensional FD-TD algorithm is computed simultaneously for the transverse magnetic (TM) case. On the boundary of the test domain Ω_T a test RBC is applied. Each point in Ω_T has a corresponding member in the substantially larger domain Ω_B. A line source is located at grid position (50, 25) in both domains. The source produces outward propagating, cylindrical waves which are spatially coincident in both domains up until time steps when the waves interact with the boundary of Ω_T. Any reflection from the boundary of Ω_T makes the solution at points within Ω_T differ from the solution at corresponding points within Ω_B. The wave solution at points within Ω_B represents the desired numerical modeling of free-space propagation up until time steps when reflections from its own boundary enter the region of Ω_B corresponding to Ω_T. By calculating the difference in the solutions in Ω_B and Ω_T at each point at each time step, a measure of the spurious reflection caused by the boundary of Ω_T is obtained.

We define at the nth time step

$$D(i, j) = E_z^T(i, j) - E_z^B(i, j) \tag{40a}$$

for all (i, j) within the test domain, where E_z^T is the solution

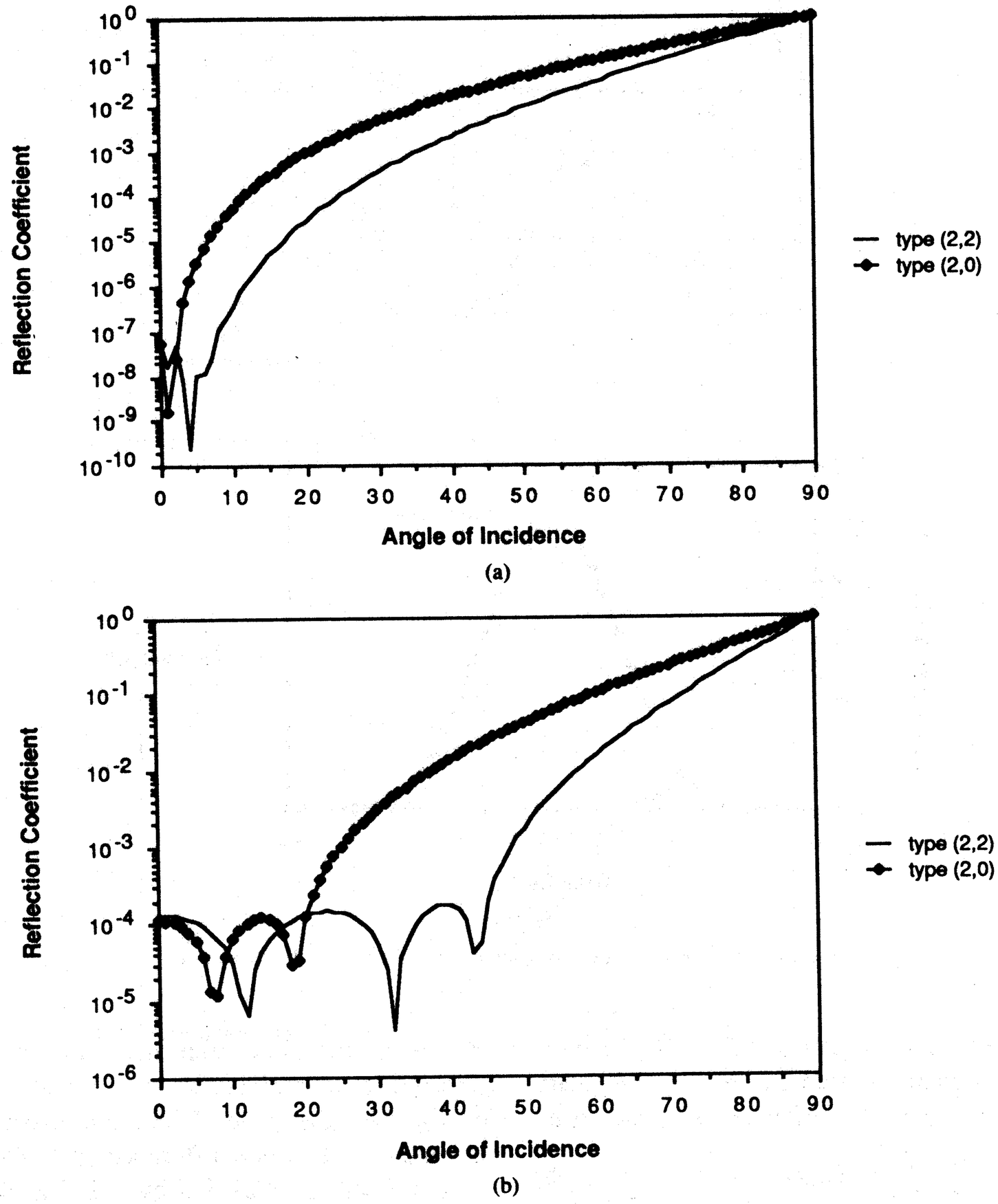

Fig. 2. Reflection coefficient versus wave angle of incidence. (a) Padé RBC. (b) Chebyshev on subinterval RBC.

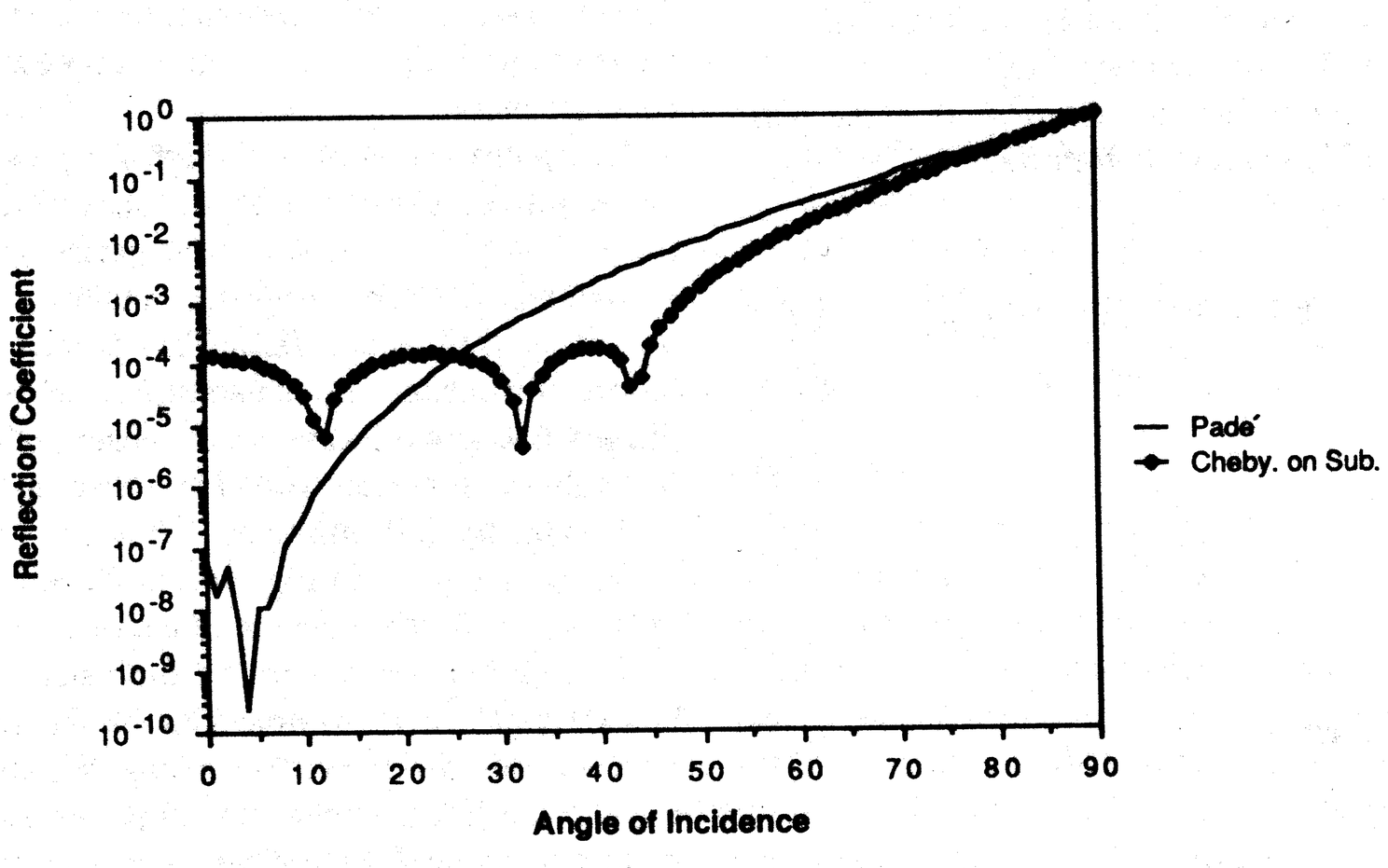

Fig. 3. Comparison of third-order RBC's.

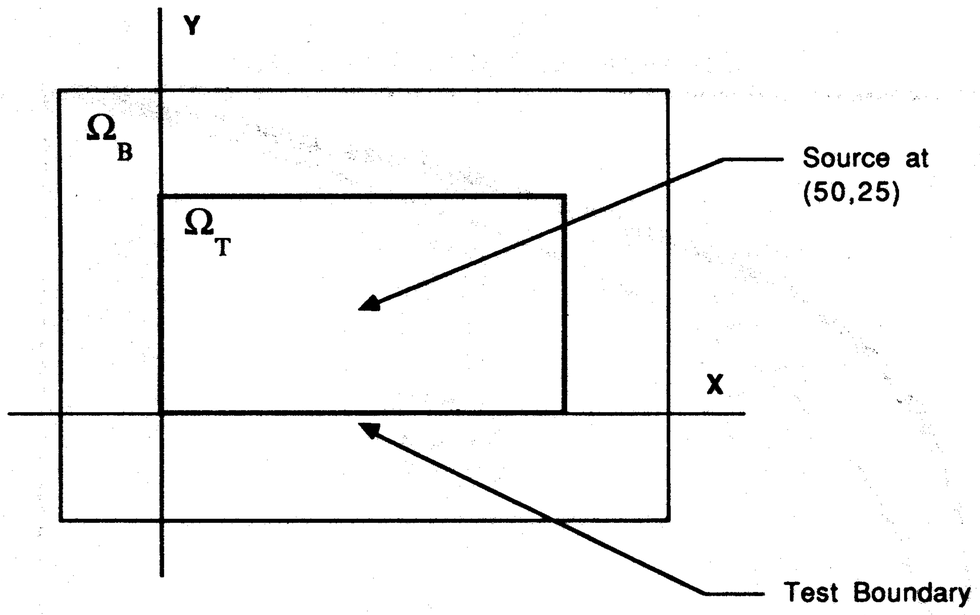

(a)

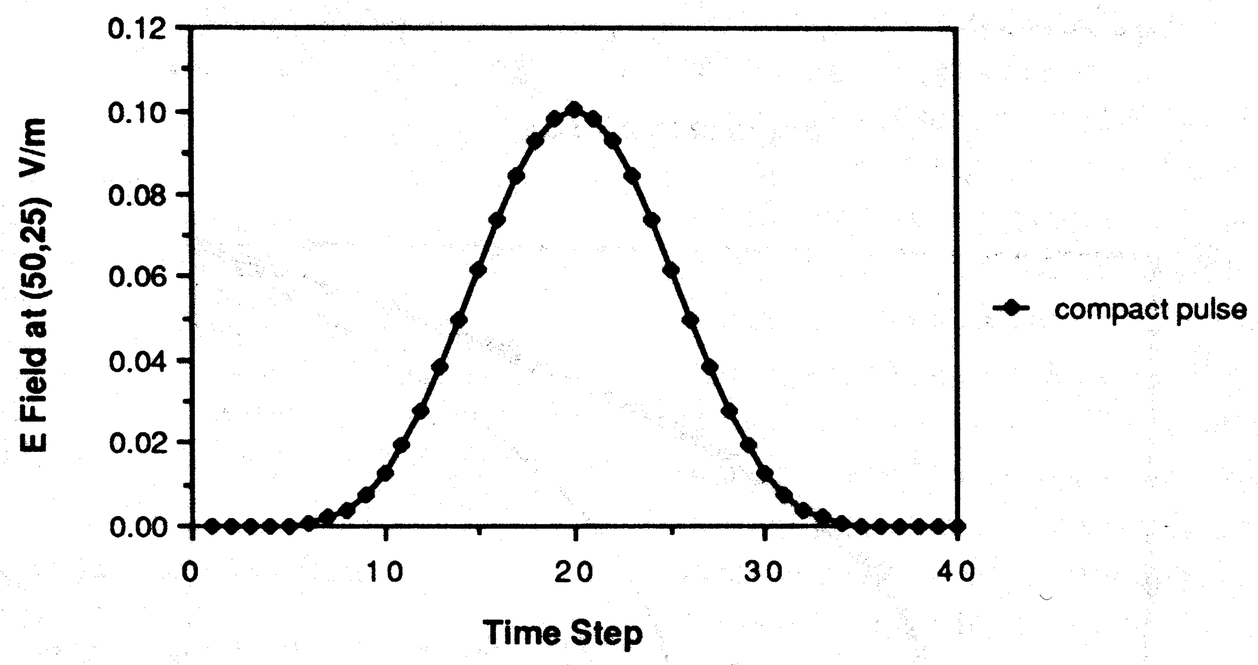

(b)

Fig. 4. Pulse studies. (a) Computational domains. (b) Wave source.

within Ω_T and E_z^B is the solution at points in Ω_B. $D(i, j)$ is the local error in the test domain caused by its grid boundary reflections. We also define a global reflected error measure,

$$E = \sum_i \sum_j D^2(i, j) \tag{40b}$$

for all (i, j) within Ω_T, which measures the total reflected error within the test grid at the nth time step.

The source used in the numerical experiments is the pulse obtained from [20] and is defined as follows:

$$E_z(50, 25, n) = \begin{cases} \alpha(10 - 15\cos\omega_1\xi + 6\cos\omega_2\xi - \cos\omega_3\xi), & \xi \le \tau \\ 0, & \xi > \tau \end{cases} \tag{41a}$$

where

$$\alpha = \frac{1}{320}$$

$$\omega_m = \frac{2\pi m}{\tau}, \qquad m = 1, 2, 3$$

$$\xi = n\delta t$$

$$\tau = 10^{-9} \tag{41b}$$

and δt is the time step used in the simulation. In all experiments we maintained $\delta t = 2.5 \times 10^{-11}$ sec and $\Delta = 2c\,\delta t$, where c is the speed of light in free-space and Δ is the space increment of the finite difference grid. The time profile of the pulse defined in (41a) is shown in Fig. 4(b). This pulse was selected because it has an extremely smooth transition to zero. As discussed in [20], the pulse has its first five derivatives vanish at $\xi = 0, \tau$ and is a good approximation to a smooth compact pulse.

This pulse has very little high-frequency content which is important because of the deleterious effects of grid dispersion (dependence of numerical wave phase velocity upon spatial wavenumber). Grid dispersion and its relation to RBC's is discussed in [21], and [22]. This problem is compounded in higher dimensions by anisotropies of the numerical wave phase velocity with wave vector angle in the grid [3], [23] and is a subject of current research aimed at further reduction of grid boundary reflection coefficients.

The source point in Fig. 4(a) is 25 cells from the boundary of Ω_T at $y = 0$. With the specification $\Delta = 2c\,\delta t$, disturbances at the source point require 50 time steps to propagate to the boundary at $y = 0$. At time step 70, the peak of the pulse just starts to pass through the boundary. We choose to observe the reflection at the first row of grid points away from the $y = 0$ boundary (along $J = 1$) at time step $n = 100$. This permits the bulk of the outgoing pulse to pass through the boundary and excite the largest observable reflection.

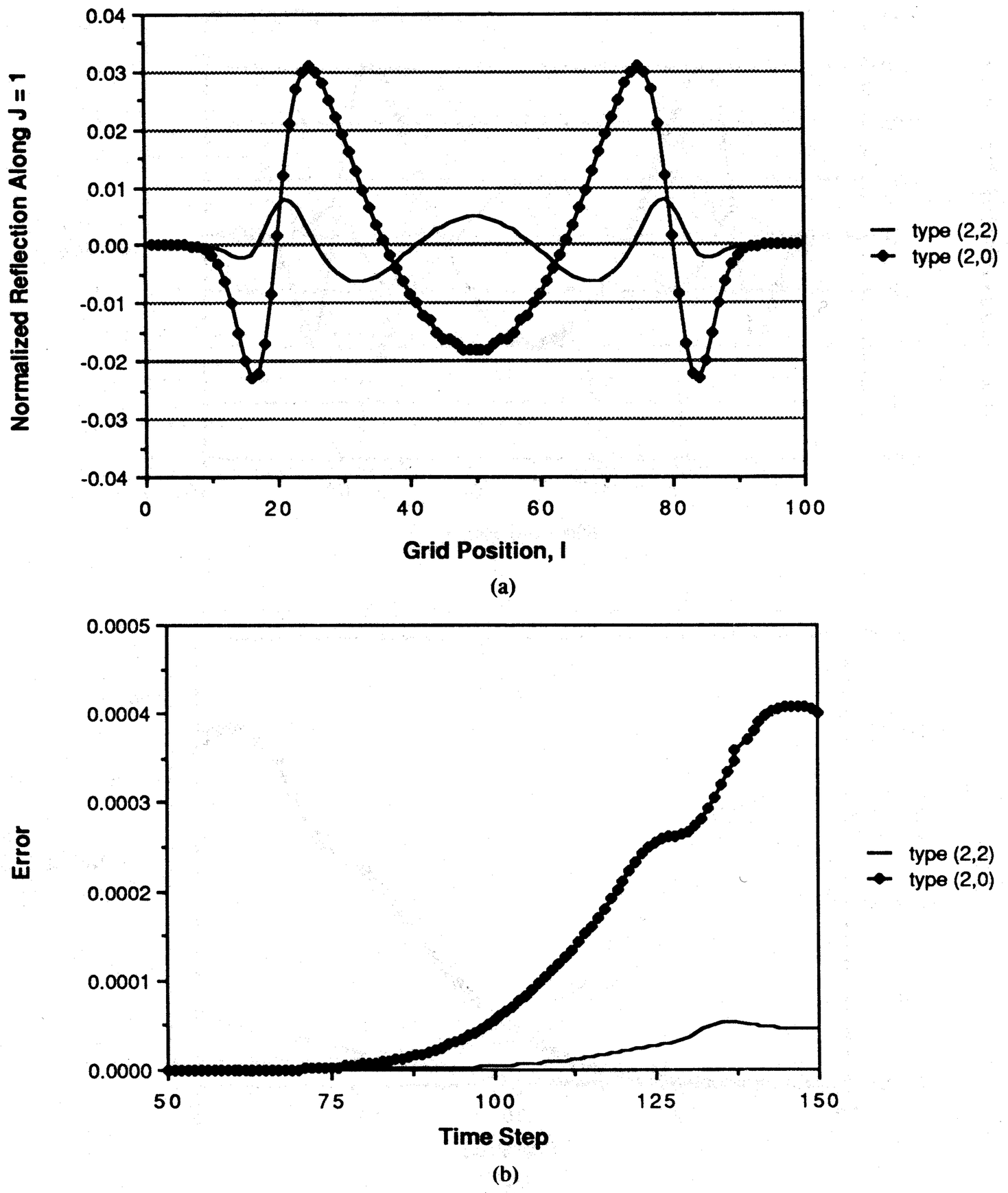

Fig. 5. Error measures, Padé RBC. (a) Local error at $n = 100$. (b) Global error.

Figs. 5 and 6 show the local and global reflection errors observed for the Padé and L_a^∞ RBC's. Fig. 7 compares the third-order conditions. In Figs. 5(a), 6(a), and 7(a), $D(i, 1)$ has been normalized with the peak value of the incident pulse which strikes the $y = 0$ boundary at time step $n = 70$ at grid position (50, 0). The pulse experiment results are in agreement with the reflection coefficient analysis by showing that higher order RBC's do perform better than lower order RBC's in actual simulations. However, comparison of the third-order L_a^∞ RBC to the third-order Padé RBC does not indicate any particular performance advantage. The improved wide-angle performance suggested in [15] is not evident in these experiments.

IV. Application of Mode-Annihilating Operators: OSRC

The on-surface radiation condition method [1] is a new analytical technique by which it is possible to construct accurate approximation of two- and three-dimensional scattering problems involving convex and simple reentrant targets. In this section, two areas of application will be examined. In the first application, the OSRC method will be applied to compute the scattering cross section of two canonical convex targets: 1) a circular cylinder illuminated by both a transverse electric (TE) and transverse magnetic polarized plane wave; and 2) an acoustic sphere with a constant surface impedance. In the second application, the OSRC method will be applied to the scattering of a plane wave by a canonical reentrant geometry: the open end of a semi-infinite flanged parallel-plate waveguide. Before either of the cases is examined, some background discussion on the OSRC method is necessary.

A. Background

The OSRC method is based upon the application of a radiation boundary operator, such as those discussed in Section II, directly on the surface of the target. The effect of this is to relate the surface currents to known field quantities through a simple expression; thus the problem reduces to solving an equation along the contour of the target. Only second-order operators will be considered here because they are the most widely used. The method used in this paper will be the same one used in [1]. For completeness, recently proposed variations will be reviewed as well.

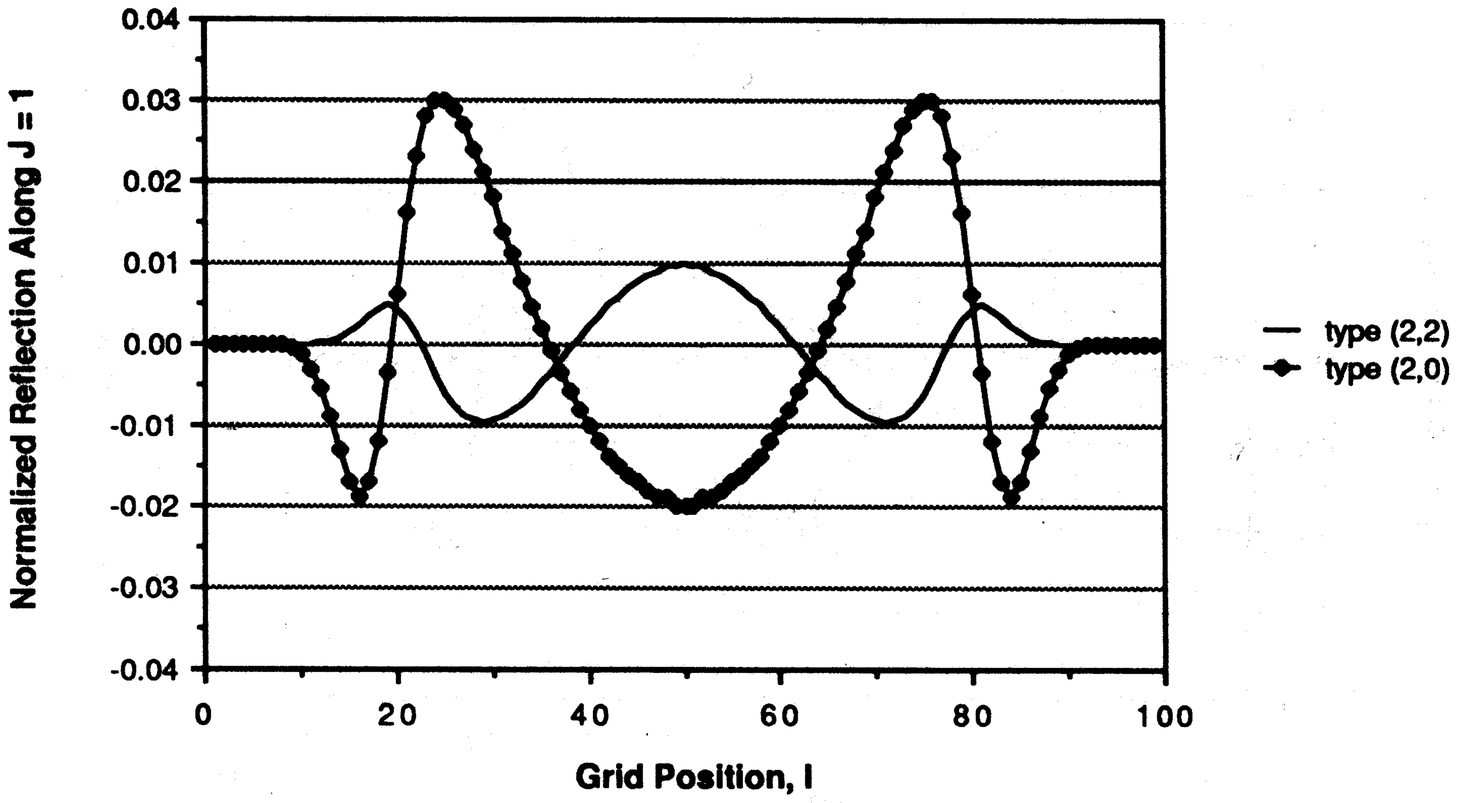

Fig. 6. Error measures, Chebyshev on subinterval RBC. (a) Local error at $n = 100$. (b) Global error.

The original method developed for two-dimensional electromagnetic targets is to apply a mode-annihilating radiation boundary operator locally at each point on the surface of the target [1]. This is conveniently done by noting that an osculating circle can approximate the target's surface locally at each point. The operator then works on the fields as if they were emanating from within the local osculating circle. In two dimensions, this is accomplished by making the following substitutions:

$$\frac{\partial}{\partial r} \rightarrow \frac{\partial}{\partial n} \tag{42a}$$

$$\frac{1}{r} \rightarrow \kappa(s) \tag{42b}$$

$$\frac{1}{r^2}\frac{\partial^2}{\partial \theta^2} \rightarrow \frac{\partial^2}{\partial s^2} \tag{42c}$$

where n is the outward normal, s is an arc length parameter, and $\kappa(s)$ is the curvature of the target at s. This produces the second-order two-dimensional surface boundary operator [1]

$$2(\kappa - jk)\frac{\partial}{\partial n} U = \frac{\partial^2}{\partial s^2} U + \left[2k^2 - \frac{3}{4}\kappa^2 + 3jk\kappa\right] U. \tag{42d}$$

A three-dimensional surface boundary operator developed for acoustic targets is presented in [24]. There, the following substitutions are made in the three-dimensional mode-annihilating radiation boundary operator:

$$\frac{\partial}{\partial R} \rightarrow \frac{\partial}{\partial n} \tag{43a}$$

$$\frac{1}{R} \rightarrow H(s) \tag{43b}$$

$$\frac{\nabla^2 s}{R^2} \rightarrow \nabla \cdot \nabla \tag{43c}$$

where $\nabla \cdot \nabla$ is the surface Laplacian and H is the mean curvature. This produces the second-order three-dimensional

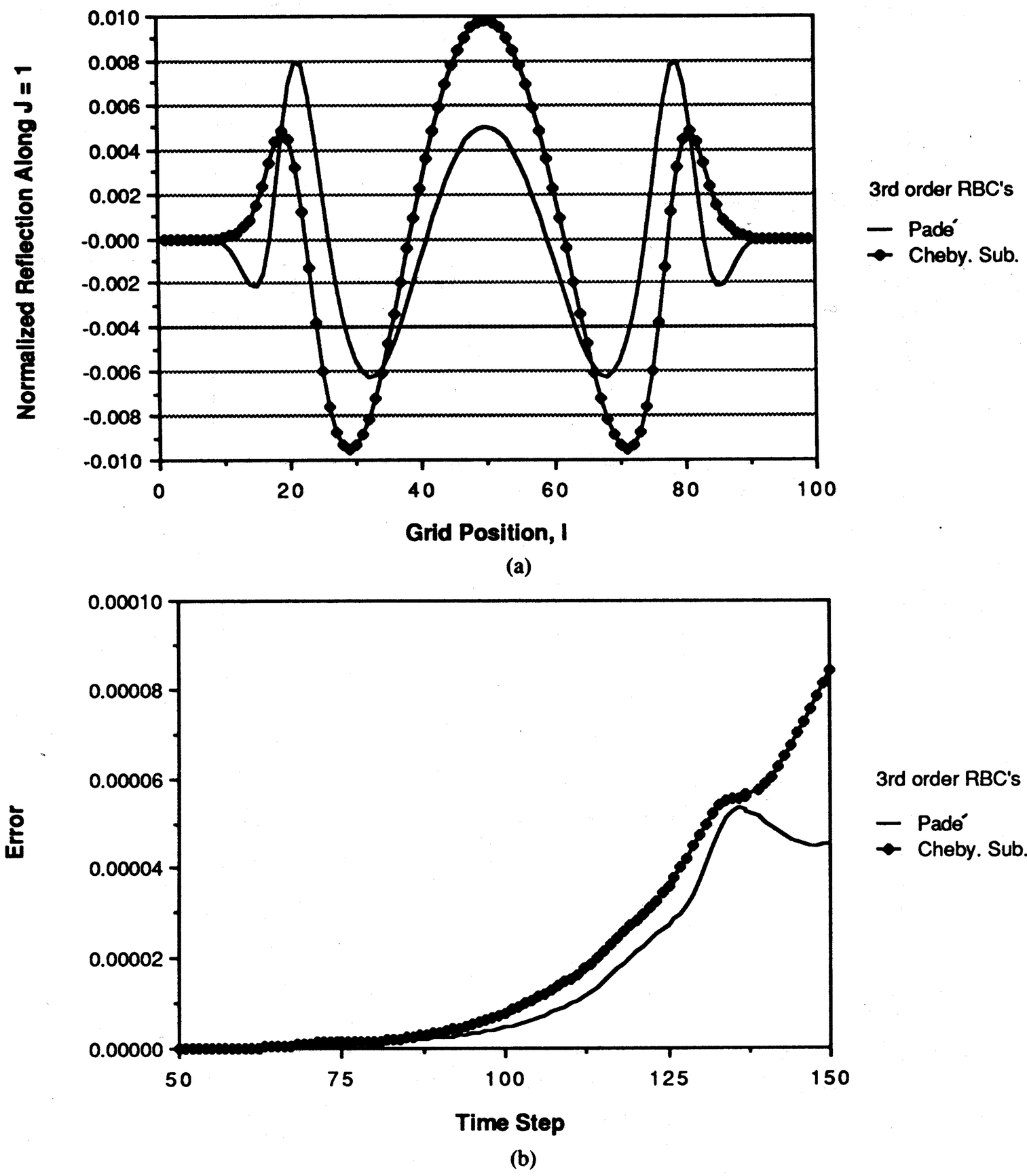

Fig. 7. Comparison of Padé to Chebyshev on subinterval. (a) Local error at $n = 100$. (b) Global error.

surface boundary operator,

$$-2jk\frac{\partial}{\partial n}U=\nabla\cdot\nabla U+2(-k^2-jkH)U. \quad (43d)$$

A variation of this surface boundary condition is presented in [25] in which a slightly different radiation boundary operator is used. It is

$$2(H-jk)\frac{\partial}{\partial n}U=\nabla\cdot\nabla U+2(H^2-k^2-2jkH)U. \quad (43e)$$

The fundamental difference between (43d) and (43e) is that the latter annihilates terms of order $(kR)^{-5}$ as compared to $(kR)^{-2}$ for the former.

Other methods have recently been presented for deriving a general surface boundary condition for OSRC. A sequence of surface boundary operators is derived in [26] by directly factoring the wave equation, as in Section II-B but in a general coordinate system based on the local properties of the target's surface. These results differ from (42d), (43d), and (43e) by a term proportional to the derivative of the curvature multiplied by k^{-2}. No published evidence exists at this time to indicate that this term has any beneficial effects. The most recent derivation of surface boundary conditions for OSRC was presented in [27], which demonstrates that the surface boundary condition can be derived directly from geometrical acoustics/optics by making the assumption that the surface of the target is a phase front. The resulting boundary condition in three dimensions is

$$2jk\frac{\partial}{\partial n}U=\nabla\cdot\nabla U+(2k^2+H^2-\kappa_G-jkH)U \quad (44a)$$

where κ_G is the Gaussian curvature. The corresponding surface boundary condition in two dimensions is

$$2(\kappa-jk)\frac{\partial}{\partial n}U=\frac{\partial^2}{\partial s^2}U+\left[2k^2-\frac{3}{4}\kappa^2+3jk\kappa\right]U - \frac{j}{4k}\frac{\partial^2\kappa}{\partial s^2}U-\frac{j}{k}\frac{\partial\kappa}{\partial s}\frac{\partial U}{\partial s}. \quad (44b)$$

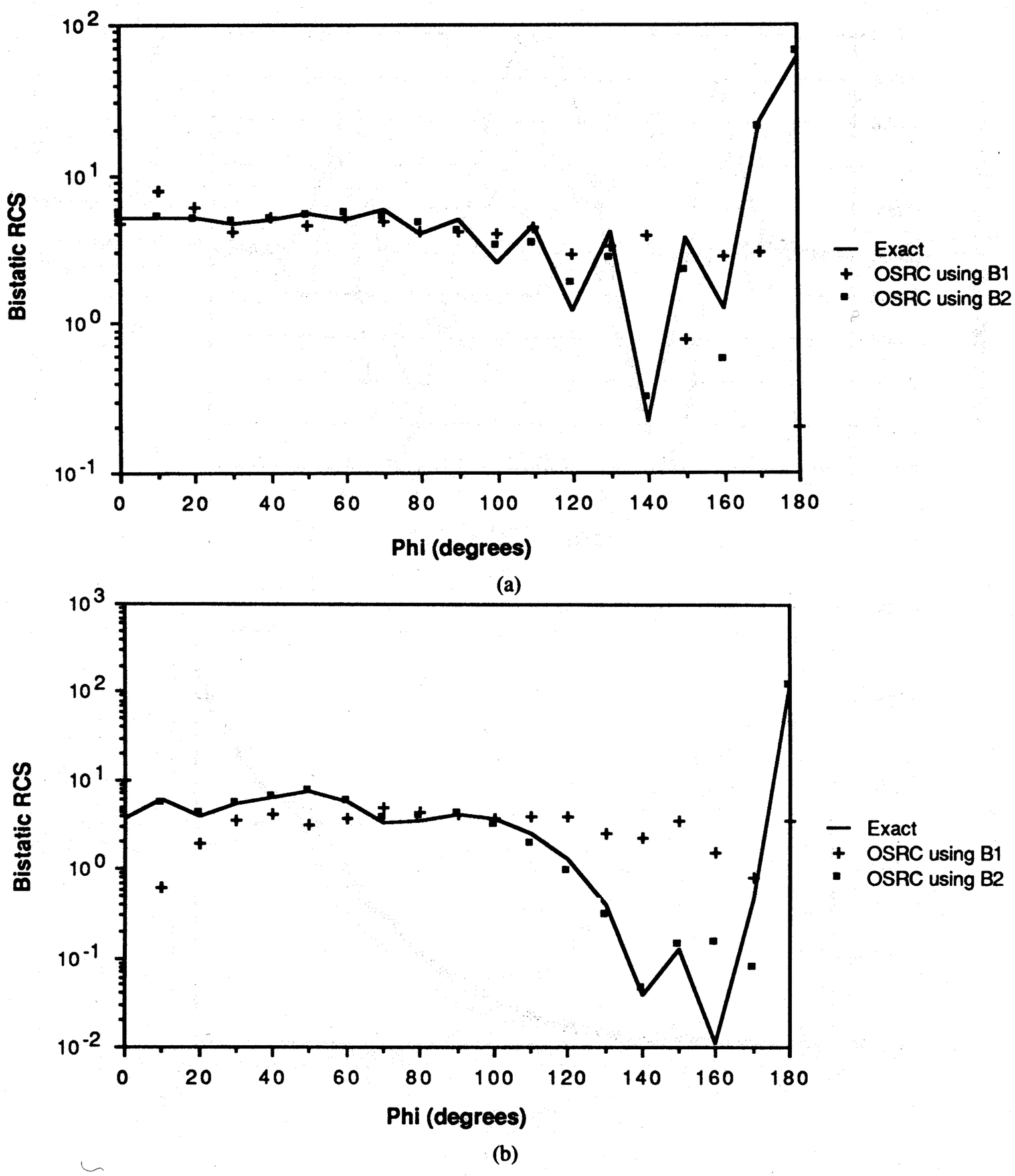

Fig. 8. OSRC computed bistatic RCS of conducting circular cylinder, TE case. (a) $ka = 10$. (b) $ka = 20$.

We note that (44b) also differs from (42d) in the terms proportional to the derivative of the target's curvature (which are formally $O(k^{-3})$ corrections), but, in turn, differs slightly from the operator derived in [26]. More importantly, [27] shows how this method is deriving surface boundary operators can be applied to the vector scattering case of OSRC. However, no validations have been published to date.

Now that the surface boundary conditions have been derived, the application of the OSRC method to scalar problems is straightforward. We set

$$B_n^s U^{scat} = 0 \tag{45}$$

on the surface of the target, where B_n^s is one of the surface boundary conditions described above. What results is an expression that relates the scattered field to its normal derivative at each point on the surface of the target. This is now combined with the usual relation between the incident and scattered field (or the normal derivative of the scattered field), as dictated by the problem.

B. Application to Scattering from Convex Targets

The use of OSRC is first illustrated by modeling scattering by a perfectly conducting circular cylinder of radius a. The cylinder is illuminated by either a transverse electric or transverse magnetic polarized plane wave. For either polarization, the second-order surface boundary condition (42d) is applied to the surface of the cylinder.

For TE polarization, with the magnetic field tangent to the target's surface, the OSRC method results in an ordinary differential equation (ODE) for the azimuthal surface current density J_ϕ:

$$C_2 \frac{d^2 J_\phi}{d\phi^2} - J_\phi = U_{\text{inc}}(1 - C_1 \cos\phi) - C_2 \frac{\partial^2 U_{\text{inc}}}{\partial \phi^2} \tag{46a}$$

where

$$C_1 = \frac{(8k^2 + j8k)}{-3 + 8k^2 + j12k} \qquad C_2 = \frac{-4}{-3 + 8k^2 + j12}. \tag{46b}$$

This is a very simple ODE since it has constant coefficients and thus may be solved analytically. The bistatic radar cross section patterns for a $ka = 10$ and $ka = 20$ cylinder, computed via a modal solution of (46), are plotted in Figs. 8(a) and (b). The OSRC results for the B_2 operator are seen to demonstrate excellent agreement with the exact solution over a

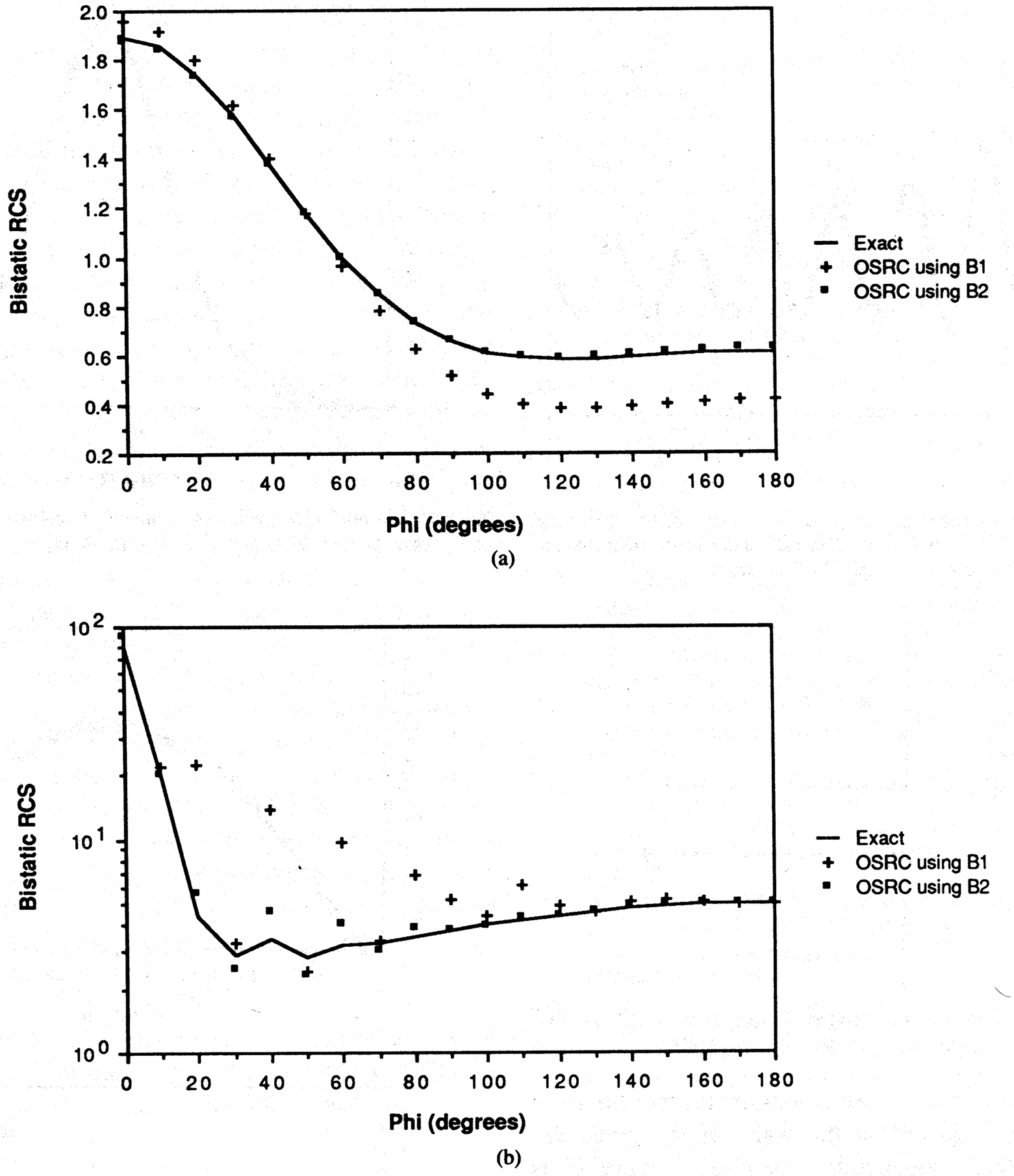

Fig. 9. OSRC computed bistatic RCS of conducting circular cylinder, TM case. (a) $ka = 1$. (b) $ka = 10$.

wide (30 dB) dynamic range. The solution to (46) can be accurately approximated by using the WKBJ method for $k \geq 5$ [28]. There an approximate formula for an arbitrary convex target is derived by the same technique.

For TM polarization, the electric field is tangent to the target's surface and thus the OSRC method gives a simple algebraic expression for the longitudinal surface current density J_z:

$$J_z = \frac{j}{\eta_0 k}\left[\frac{1}{2} + jk\,(\cos\phi - 1) - jk - \frac{j}{8k} - \frac{1}{2}\cos\phi + \frac{jk}{2}\sin^2\phi\right] e^{jk\cos\phi}. \quad (47)$$

The OSRC predicted bistatic radar cross section patterns for a $ka = 1$ and $ka = 10$ cylinder are plotted in Fig. 9(a) and (b). The OSRC results for the B_2 operator are again seen to demonstrate excellent agreement with the exact solution over a substantial dynamic range.

The application of OSRC to a basic three-dimensional convex target was first illustrated by modeling scattering by a soft acoustic sphere [24]. It was next applied to an acoustic sphere loaded with a constant impedance. Because this problem is solved in [25], only one example is presented here. In this example, an acoustic plane wave propagating in the $-z$ direction impinges upon a spherical target of radius a having a constant normalized surface impedance of $Z = 10$. Condition (43e) is applied to the surface of the sphere. After inserting (43e) into (45), a second-order partial differential equation results for the surface currents, whose solution is approximated by a simple two-term asymptotic expansion and is then used to determine the far fields. Fig. 10 shows the backscattered cross section versus k. Again, there is excellent agreement with the exact solution.

C. Application to Scattering from Reentrant Structures

The second area of application illustrates using OSRC to model scattering by simple reentrant structures. We consider the problem of a plane wave impinging on the open end of a semi-infinite flanged parallel-plate waveguide [29], shown in Fig. 11. A plane wave, at an angle α measured counterclock-

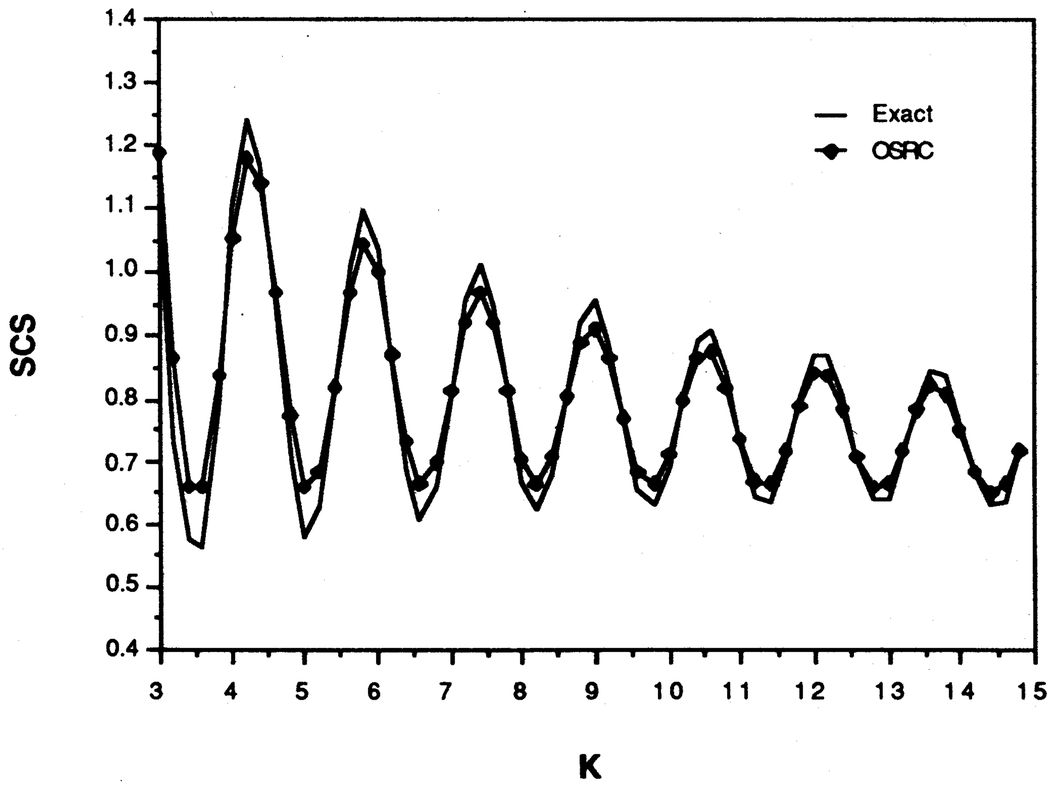

Fig. 10. Normalized back scattering cross section versus K for reactively loaded sphere ($Z = 10$). Exact solution is calculated from modal series representation. Dotted line is two-term OSRC solution.

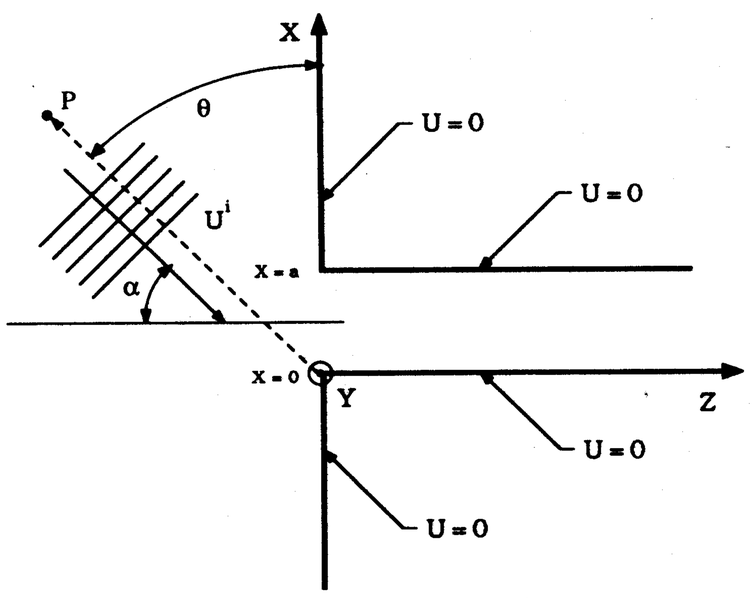

Fig. 11. Plane wave incident on open end of flanged, semi-infinite parallel-plate waveguide. $a = 1.5$ m, $f = 250$ MHz.

wise with reference to the $-z$ axis, illuminates the mouth of the waveguide. The flange and the walls of the guide are assumed to be perfectly conducting. The incident wave U^i is considered to be the y component E_y of the incident electric field vector. Thus, for the boundary conditions shown, TE modes are excited inside the guide. The operator (42d), with $\kappa = 0$, is applied to the field representations valid in the guide aperture and yields an expression for the coefficients in the modal representation of the waveguide fields. Knowledge of the modal coefficients then permits the derivation of a simple expression for the bistatic radar cross section of the field scattered by the aperture, and the fields penetrating into the waveguide. Results of calculations using this approach are presented in Figs. 12 and 13. Fig. 12 shows the bistatic cross section for a plane wave at $\alpha = 0°$. Fig. 13 show the magnitude and phase distribution of the field penetrating the guide at a distance of $z = 2$ m from the aperture. The OSRC results are compared to results obtained by FD-TD simulations. Excellent agreement is observed. The value of the OSRC solution is striking in its simple form and negligible computational requirements.

V. Future Research

Research on radiation boundary operators is presently directed at two basic goals. The first is the development of

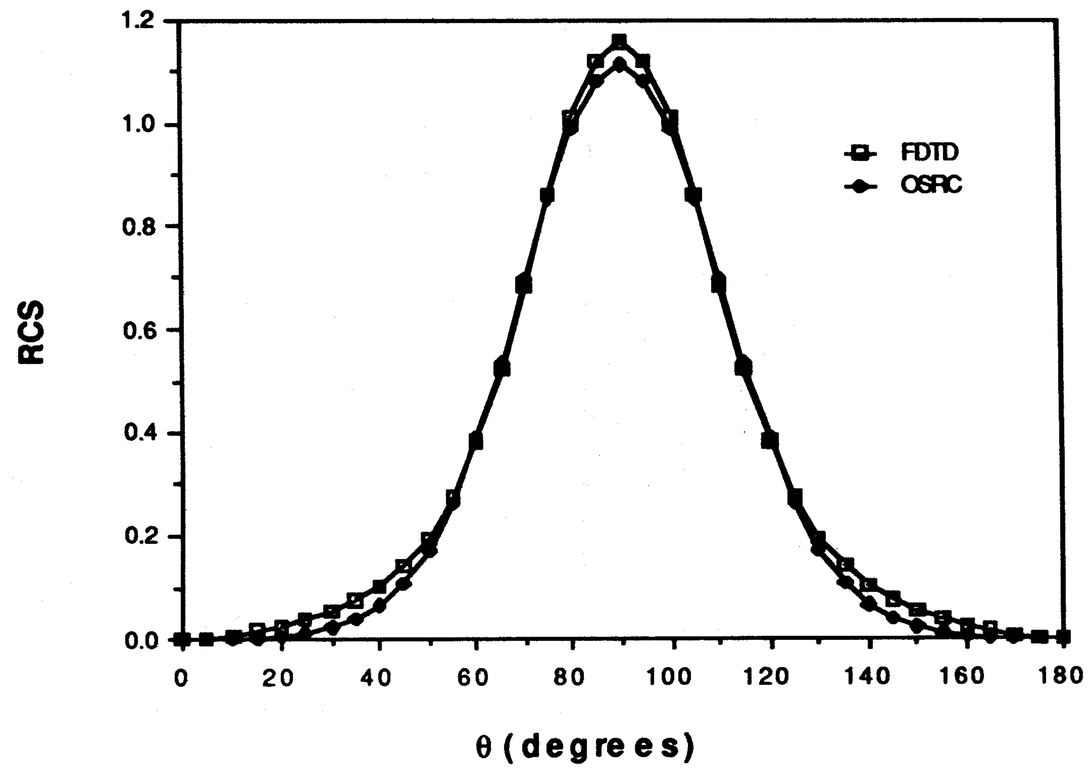

Fig. 12. Bistatic cross section for scattering from waveguide aperture due to plane wave at $\alpha = 0°$ and $f = 250$ MHz. Angle θ is as shown in Fig. 11.

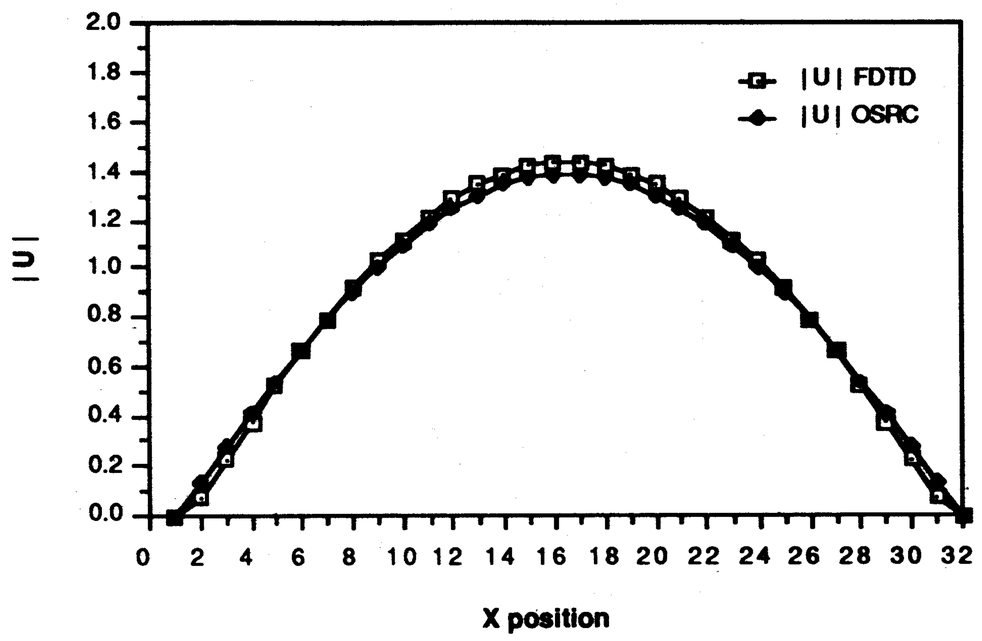

(a)

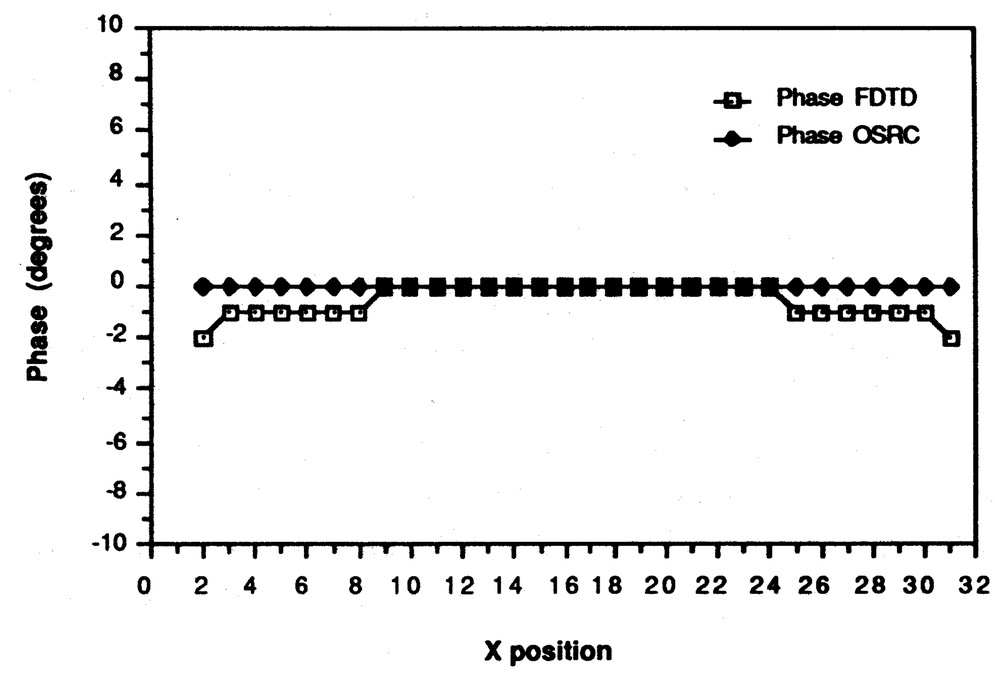

(b)

Fig. 13. Field penetration into waveguide at $z = 2$ m for plane wave at $\alpha = 0°$ and $f = 250$ MHz. (a) E-field magnitude. (a) E-field phase.

better truncation conditions for finite-difference and finite-element grids. This is aimed at reducing nonphysical reflections from the outer grid boundary which contribute to the numerical noise floor of the modeling procedure. Reducing the numerical noise floor will allow the simulation of scatterers with wider dynamic range. The second goal is the development of optimal mode-annihilating radiation boundary operators for the OSRC method.

The work on operators for truncating FD-TD and FE-TD grids fall into two basic categories. The first category is the synthesis of wide-angle radiation boundary operators. Although there are two basic types of radiation boundary operators, the main thrust of the research is directed towards one-way wave equation approximations. Here, work is proceeding in deriving approximations to the dispersion relation that will absorb waves over a wide range of angles properly taking into account anisotropy and dispersion of numerical mode phase velocities. The second category concerns the difference approximation for the operator. This is crucial for the operation of the boundary condition, because a perfectly valid operator which is not properly converted to a finite-difference equation, may cause instabilities in the simulation.

In contrast to the work on the grid truncation operators, the work on surface boundary conditions for the OSRC method is based on the optimization of the mode-annihilating radiation boundary operators. A key goal of this research is to produce a surface boundary condition which can better predict tangential energy propagation along the target's surface. Presently, two methods are being investigated for this purpose. The first method postulates a special multiplicative operator that models tangential propagating waves. The second method depends upon the application of the OSRC in the time domain to obtain a target impulse response [30]. The idea is to adjust the coefficients in the operator to match the exact response over a wide frequency range. Finally, the operators are also being examined to assess their ability to predict the correct current singularities on targets with edges.

Acknowledgment

The authors wish to acknowledge the contributions of Professor Korada R. Umashankar of the University of Illinois at Chicago in the development of the OSRC theory.

References

[1] G. A. Kriegsmann, A. Taflove, and K. R. Umashankar, "A new formulation of electromagnetic wave scattering using an on-surface radiation boundary condition approach," *IEEE Trans. Antennas Propagat.*, vol. AP-35, pp. 152–161, Feb. 1987.

[2] A. Taflove and K. R. Umashankar, "The finite-difference time-domain (FD-TD) method for electromagnetic scattering and interaction problems," *J. Electromagn. Waves Appl.*, vol. 1, no. 4, pp. 363–387, 1987.

[3] A. C. Cangellaris, C. C. Lin, and K. K. Mei, "Point-matched time-domain finite-element methods for electromagnetic radiation and scattering," *IEEE Trans. Antennas Propagat.*, vol. AP-35, pp. 1160–1173, Oct. 1987.

[4] A. Sommerfeld, *Partial Differential Equations in Physics.* New York: Academic, 1949.

[5] G. A. Kriegsmann and C. S. Morawetz, "Numerical solutions of exterior problems with the reduced wave equation," *J. Comput. Phys.*, vol. 28, pp. 181–197, 1979.

[6] A. Bayliss and E. Turkel, "Radiation boundary conditions for wave-like equations," *Commun. Pure Appl. Math.*, vol. 23, pp. 707–725, 1980.

[7] F. G. Friedlander, "On the radiation field of pulse solutions of the wave equation," *Proc. Royal Soc. London Ser. A*, vol. 269, pp. 53–69, 1962.

[8] C. H. Wilcox, "An expansion theorem for electromagnetic fields," *Commun. Pure Appl. Math.*, vol. 9, pp. 115–132, 1956.

[9] A. Bayliss, M. Gunzburger, and E. Turkel, "Boundary conditions for the numerical solution of elliptic equations in exterior regions," *SIAM J. Appl. Math.*, vol. 42, pp. 430–451, Apr. 1982.

[10] S. N. Karp, "A convergent far-field expansion for two-dimensional radiation functions," *Commun. Pure Appl. Math.*, vol. 14, pp. 427–434, 1961.

[11] B. Engquist and A. Majda, "Absorbing boundary conditions for the numerical simulation of waves," *Math. Comput.*, vol. 31, pp. 629–651, July 1977.

[12] L. Halpern and L. N. Trefethen, "Wide-angle one-way wave equations," Dept. Math., Mass. Inst. Technol., Cambridge, Numerical Analysis Rep. 86-5, July 1986.

[13] G. Mur, "Absorbing boundary conditions for the finite-difference approximation of time-domain electromagnetic field equations," *IEEE Trans. Electromagn. Compat.*, vol. EMC-23, pp. 377–382, Nov. 1981.

[14] K. R. Umashankar and A. Taflove, "A novel method to analyze electromagnetic scattering of complex objects," *IEEE Trans. Electromagn. Compat.*, vol. EMC-24, pp. 392–405, Nov. 1982.

[15] L. N. Trefethen and L. Halpern, "Well-posedness of one-way wave equations and absorbing boundary conditions," *Math. Comput.*, vol. 47, pp. 421–435, Oct. 1986.

[16] J. G. Blaschak and G. A. Kriegsmann, "A comparative study of absorbing boundary conditions," *J. Comput. Phys.*, vol. 77, pp. 109–139, July 1988.

[17] G. B. Whitham, *Linear and Nonlinear Waves.* New York: Wiley, 1974.

[18] R. L. Higdon, "Absorbing boundary conditions for difference approximations to the multidimensional wave equation," *Math. Comput.*, vol. 47, pp. 437–459, 1986.

[19] ——, "Numerical absorbing boundary conditions for the wave equation," *Math. Comput.*, vol. 49, pp. 65–90, 1987.

[20] G. A. Kriegsmann, A. N. Norris, and E. L. Reiss, "Acoustic pulse scattering by baffled membranes," *J. Acoust. Soc. Amer.*, vol. 79, Jan. 1986.

[21] L. N. Trefethen, "Group velocity in finite difference schemes," *SIAM Rev.*, no. 24, pp. 114–136, 1982.

[22] ——, "Group velocity interpretation of stability theory of Gustafasson, Kreiss, and Sundstrom," *J. Comput. Phys.*, no. 49, pp. 199–217, 1983.

[23] A. Taflove and K. R. Umashankar, "Advanced numerical modeling of microwave penetration and coupling for complex structures—Final report," Lawrence Livermore National Lab., VCRL-15960, Contract 6599805, Sept. 1987.

[24] D. S. Jones, "An approximate boundary condition in acoustics," submitted to *J. Sound Vibration,* 1987.

[25] G. A. Kriegsmann and T. G. Moore, "An application of the on-surface radiation condition to the scattering of acoustic waves by a reactively loaded sphere," *Wave Motion*, vol. 10, pp. 277–284, 1988.

[26] W. F. Richards, D. R. Wilton, and J. X. Jiang, "Factorization of the three-dimensional Helmholtz equation with applications to the on surface radiation condition method," submitted to *IEEE Trans. Antennas Propagat.*, 1987.

[27] D. S. Jones, "Surface radiation conditions," submitted to *IMA J. Appl. Math.*, 1987.

[28] T. G. Moore, G. A. Kriegsmann, and A. Taflove, "An application of the WKBJ technique to the on-surface radiation condition," *IEEE Trans. Antennas Propagat.*, vol. 36, pp. 1329–1331, Sept. 1988.

[29] J. G. Blaschak, G. A. Kriegsmann, and A. Taflove, "A study of wave interactions with flanged waveguides and cavities using the on-surface radiation condition method," *Wave Motion*, in press.

[30] T. G. Moore, G. A. Kriegsmann, and A. Taflove, "An application of the OSRC method to time dependent problems," submitted to *IEEE Trans. Antennas Propagat.*, 1988.

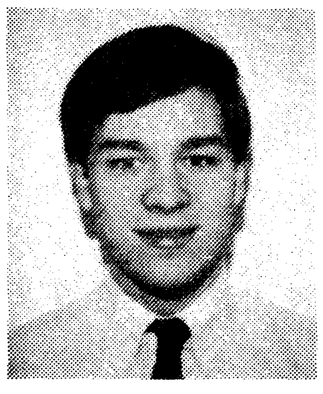

Thomas G. Moore (S'84) received the B.S. and M.S. degrees in 1986 and 1987, respectively, from Northwestern University, Evanston, IL, where he is currently working toward the Ph.D. degree.

His research interests include computational electromagnetics, electromagnetic theory, and nonlinear wave propagation.

Mr. Moore is a member of Tau Beta Pi and Eta Kappa Nu.

Jeffrey G. Blaschak (S'84) received the B.S. degree from the University of Pittsburgh, Pittsburgh, PA, the M.S. degree from Purdue University, Lafayette, IN, and the Ph.D. degree in electrical engineering from Northwestern University, Evanston, IL, in 1988.

He has worked for AT&T Bell Laboratories, Lockheed Missiles and Space Company, and the Pennsylvania State University. Currently, he is a Member of the Technical Staff at MIT Lincoln Laboratory, Lexington, MA. His research interests include various numerical techniques for the computation of electromagnetic wave propagation, radiation and scattering.

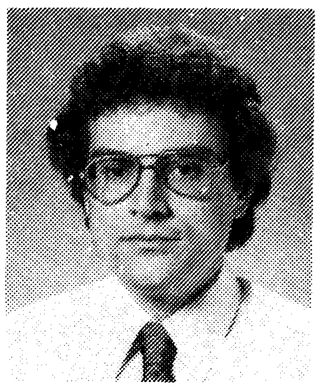

Allen Taflove (M'75–SM'84) was born in Chicago, IL, on June 14, 1949. He received the B.S. (with highest distinction), M.S. and Ph.D. degrees in electrical engineering from Northwestern University, Evanston, IL, in 1971, 1972, and 1975, respectively.

From 1975 to 1984, he was a staff member at IIT Research Institute in Chicago, IL, holding the positions of Associate Engineer, Research Engineer, and Senior Engineer. There, his research was concerned with computational modeling of electromagnetic wave penetration and scattering interactions with complex structures, power-frequency coupling of earth-return transmission systems, and development of novel techniques for recovery of oil from oil shale, tar sand, and slowly producing conventional wells based upon *in situ* radio-frequency heating. He was the principal investigator on eight externally funded programs in these areas, including five which contributed to the early development of the finite-difference time-domain numerical modeling approach for complex electromagnetic wave interaction problems. He also provided technical leadership for major field experiments in radio frequency heating applied to oil recovery and is one of three principal co-inventors of technology in this area that is now covered by more than ten U.S. patents. In 1984, he returned to Northwestern where he is now Professor of Electrical Engineering and Computer Science. He has continued research in computational electromagnetics and related areas, including inverse scattering and target synthesis; propagation and scattering of waves within dispersive, nonlinear, and time-varying media; and applications of vector and concurrent-processing supercomputers to numerical electromagnetics. A recent research topic of great interest is the on-surface radiation condition approach for scattering.

Dr. Taflove is a member of Tau Beta Pi, Eta Kappa Nu, and Sigma Xi, and is a member of Commission B of URSI. He was senior author of a paper awarded the Best Paper prize at the IEEE 1983 International Symposium on Electromagnetic Compatibility, Washington, DC.

Gregory A. Kriegsmann, for a photograph and biography see page 161 of the February 1987 issue of this TRANSACTIONS.